PERGAMON

International Journal of Heat and Mass Transfer 45 (2002) 4107–4115

International Journal of HEAT and MASS TRANSFER

www.elsevier.com/locate/ijhmt

Critical heat flux correlation for subcooled boiling flow in narrow channels

M. Kureta *, H. Akimoto

Tokai Research Establishment, Japan Atomic Energy Research Institute, Tokai, Naka, Ibaraki 319-1195, Japan

Received 10 August 2001; received in revised form 26 March 2002

Abstract

The purpose of this study is to conduct the critical heat flux (CHF) correlation for narrow channels. The CHF of subcooled flow boiling of water in narrow rectangular channels under atmospheric pressure was measured parametrically. Experimental test channels were rectangular and heated from one side with the channel gap of 0.2–3.0 mm, channel width of 7–22 mm, and heated length of 50–200 mm. First, the CHF correlation for the one-side heated rectangular channels was proposed with investigating the various system parameter effects on CHF. Next, applicability of the correlation to both-side heated rectangular channel, half-circumferentially heated tube, and full-circumferentially heated tubes was examined. New CHF correlation for narrow rectangular channels and small-diameter tubes was proposed using the critical quality, dimensionless CHF parameter and heated perimeter ratio. Calculation accuracy of the correlation is ±45% (maximum 10 times better in comparison with the existing CHF calculation methods which were proposed for the full-circumferentially heated tubes).

1. Introduction

Prediction of critical heat flux (CHF) in a narrow rectangular channel is important in relation to design of high-heat-flux components such as cooling channels of High Intensity Spallation Neutron Source (SNS) [1] and Fusion Neutron Source (FNS) [2] being planned in the Japan Atomic Energy Research Institute (JAERI). In the rotating target of FNS and solid target of SNS, a nuclear fusion reaction and a spallation reaction are generated in order to produce a high-energy neutron beam by injection of high-intensity deuteron or proton beam from one side of the cooling channel. Beam injection side on the cooling channel in the FNS rotating target becomes the high heat flux. In the case of SNS solid target, one or both sides on the cooling channel become high heat flux. For thermal-hydraulic design of these high-heat-flux components, a cooling method by water with a high mass velocity and a high subcooling has been examined. Channel gap in the FNS rotating target is designed to be approximately 0.5 mm. And the one in the SNS solid target is designed ranging from 1 to 3 mm. To best design these components, it is indispensable to predict subcooled boiling CHF in narrow rectangular channels appropriately. Up to the present, many of high-CHF researches have targeted the pipe flow [3,4]. Therefore, the applicable range of most CHF correlations [5,6] and mechanistic models [7–9] is limited in full-circumferentially heated round tubes. Mishima et al. [10] investigated the CHF in both-side heated rectangular channels with heated length of 100 mm. Kobayashi and Mishima [11] made CHF experiments using half-circumferentially heated round tube. Araki et al. [12] investigated the subcooled boiling CHF for fusion reactor components. There has been, however, no research concerning subcooled boiling CHF in one-side heated narrow rectangular channels.

The present authors performed an experimental work to correct rigorous database of the CHF in one-side

* Corresponding author. Tel.: +81-29-282-6428; fax: +81-29-282-6427.

E-mail address: kureta@hflwing.tokai.jaeri.go.jp (M. Kureta).

0017-9310/02/$ - see front matter
PII: S0017-9310(02)00129-1

Nomenclature

A	flow area (m^2)
Bo	boiling number, defined by Eq. (2) (–)
C_1	heating geometry parameter 1 defined by Eq. (4) (–)
C_2	heating geometry parameter 2 defined by Eq. (4) (–)
C^+	geometry parameter defined by Eq. (2) (–)
D_e	hydraulic equivalent diameter (m)
G	mass velocity (kg/(m^2 s))
h_{fg}	latent heat of vaporization (J/kg)
h_{fsat}	enthalpy of saturated fluid (J/kg)
h_{in}	enthalpy of fluid at the inlet (J/kg)
K^+	dimensionless CHF parameter defined by Eq. (3) (–)
L	length (m)
L_d	length of velocity developing region (m)
L_h	heated length (m)
P	pressure (Pa)
P_h	heated perimeter (m)
P_w	wetted perimeter (m)
q_{CHF}	critical heat flux (W/m^2)
s	channel gap (m)
T_{in}	inlet water temperature (°C)
u	velocity (m/s)
w	channel width (m)
w_h	width of the heated surface (m)
x_{eq}	equilibrium vapor quality (–)
x_{ex}	equilibrium vapor quality at the exit of the heated section (–)
$x_{ex,CHF}$	critical quality defined by Eq. (2) (–)
x_{in}	equilibrium vapor quality at the inlet of the heated section (–)
z	flow-directional distance from the heated inlet (m)

heated rectangular channels under subcooled boiling conditions [13] and examined the extensibility of the existing CHF correlations and models [14]. It was found from the examination that Sudo's model [8], which was already optimized using a part of the present CHF database, gave comparatively a good prediction under the condition of low inlet water temperature. On the other hand, other correlations and models are inapplicable to design the high-heat-flux components because of low prediction accuracy. Most of the correlations and models tend to overestimate the CHF, $q_{CHF,cal}/q_{CHF,exp} \fallingdotseq -100\%$ to $+500\%$. At the conceptual-design phase of each component, for example, the CHF value was determined to be about 10 times higher in value than the calculated one by Sudo's CHF model. In order to optimize the component conditions at the detailed-design phase, CHF correlation of which accuracy should be within 50% needs to be developed. And the correlation is required to be simple in form because it will be installed in the numerical analysis code as a constitutive equation in order to evaluate the safety margin of the components.

The aim of this study is to propose the CHF correlation for high-heat-flux one-side heated narrow rectangular channels. In this paper, at first, the dimensionless CHF correlation is shown while arranging the effects of various parameters on CHF. Next, the CHF correlation in one-side heated rectangular channels is attempted to apply to the both-side heated rectangular channel and small-diameter tubes. Optimization is made on the correlation to calculate the CHF in various heating geometry channels comprehensively.

2. Experimental apparatus

The experiments were detailed in the previous report [13]. In this chapter, indispensable matters concerned with the measurement of a CHF are described. Schematic of the experimental apparatus is shown in Fig. 1. Ion-exchanged water circulates in the loop. Exit pressure of the test section is atmospheric pressure. Fig. 2 shows schematic view of an example of the test section (A). The test sections are rectangular channels heated from one side and simulate the flow channel of the FNS rotating target [1]. The target in the design phase did not have a flow-developing region at the flow-inlet and flow-outlet such as a test section (A). However, such channel geometry with no flow-developing region is not general. Test section (B) shown in Fig. 3 was made in order to evaluate the effect of flow-developing region on CHF. Cross sections of the flow area in flow-developing region, heated region and flow-outlet region in the test section (B) are equal. Test sections are fixed vertically. The heater is made of copper with the thickness of 5 μm and is uniformly heated by DC power supply. Heat flux was increased stepwise to a CHF at constant inlet water temperature and mass velocity. The CHF was calculated by the current and voltage drop between the inlet and exit of the heated section at the physical burnout condition.

The experiments were carried out by changing the system parameters systematically in order to clarify the effects of geometry parameters and flow parameters on CHF. Table 1 shows the experimental conditions. As equilibrium vapor qualities at the exit of the heated section, x_{ex} were measured ranging from -0.127 to

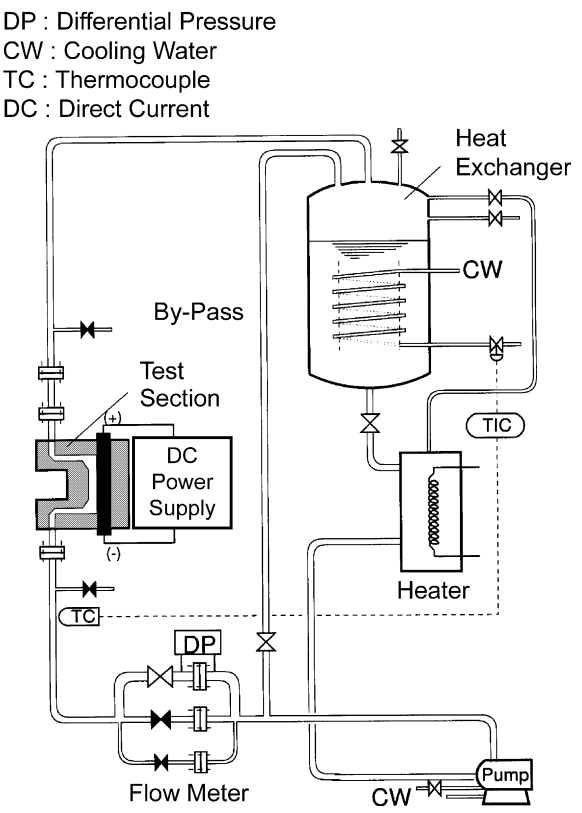

Fig. 1. Schematic diagram of the experimental loop.

-0.013, all CHF data taken by the present experiments were in the subcooled boiling region ($x_{ex} < 0$).

3. Experimental results and discussion

It was thought that the CHF measured in the test section (A) which does not have a flow-developing region indicates a peculiarity caused by the special geometry at the inlet and exit and flow profile (velocity boundary layer). At first, we investigated this peculiar geometry effect on CHF. Next, the dimensionless CHF correlation was conducted clarifying the effects of geometry and flow parameters on CHF. Measurement error and scattering of the data obtained at the same test section was $\pm 20\%$. It has been found from many kinds of CHF experiments that the CHF data tend to scatter at low pressure, low exit quality conditions and narrow channel conditions. The reason why the CHF data scattered within 20% in the present experiments may be due to the flow conditions (narrow channels, low pressure, and low quality CHF conditions) and the production accuracy of the copper-foil heaters.

3.1. Effect of flow-developing region on CHF

Test section (B) was designed as the standard test section, which has a flow-developing region with flow-developing length, L_d and flow-outlet region in order to investigate the effect of the inlet and exit geometry on CHF. In case of turbulence, it is thought that flow

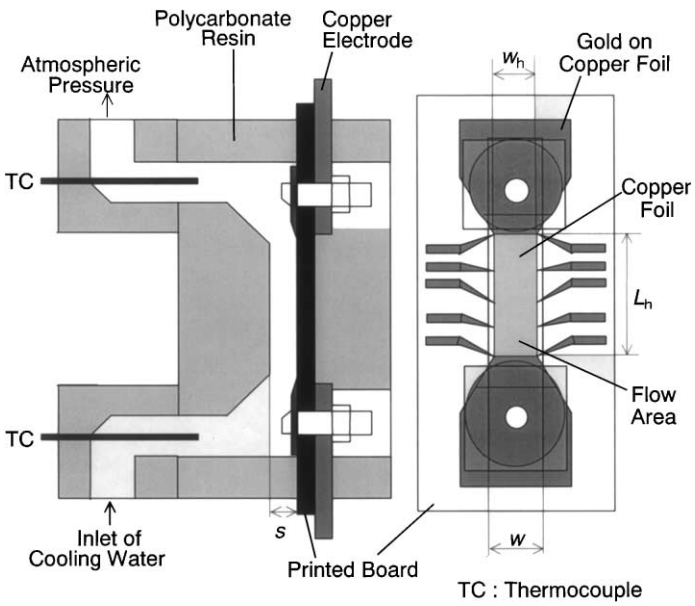

Fig. 2. Schematic view of the test section (A).

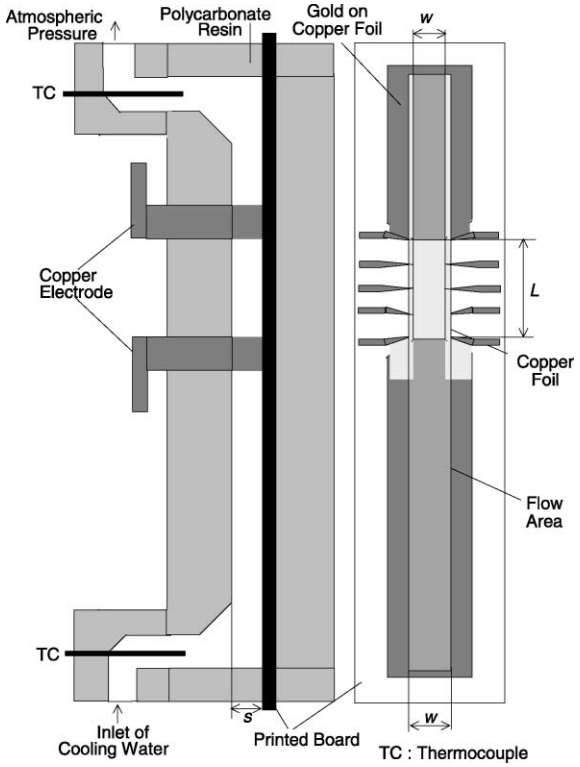

Fig. 3. Schematic view of the test section (B).

Table 1
Experimental conditions

Parameter	Symbol	Range
Channel gap	s	0.2, 0.5, 1.0, 3.0 mm
Channel width	w	7, 12, 22 mm
Heated width	w_h	5, 10, 20 mm
Heated length	L_h	50, 100, 200 mm
Equivalent diameter	D_e	4.2–5.28 mm
Inlet water temperature	T_{in}	30–90 °C
Mass velocity	G	846–15 100 kg/(m^2 s)

develops at $L_d/D_e \fallingdotseq 10$–20 point. Since the L_d/D_e of the test section (B) is 46, we estimated that flow was fully developed at the inlet of the heated section. CHF experiments were carried out using the various test sections, (A) and (B), under same cross section and inlet conditions. Obtained data was compared mutually to estimate the effect of the flow-developing region. Fig. 4 shows an example of the comparison results. Curved lines indicated in Fig. 4 represent five-dimensional least-square fitting curves of the data. It was found that the CHF increases almost linearly as a function of mass velocity and the difference between the no-developing region data and with-developing region data was small. Similar tendency could be seen in case of inlet water

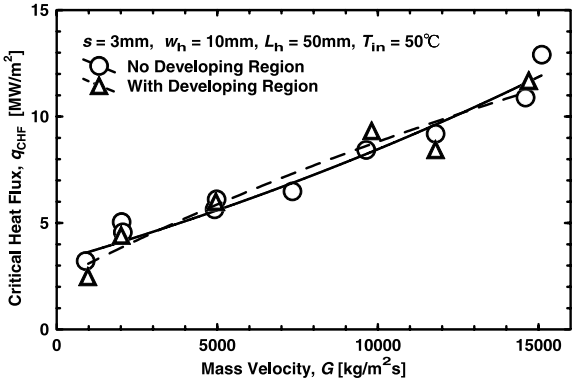

Fig. 4. Effect of the developing region on CHF.

temperature = 30, 70, and 90 °C. The effect of flow-developing region on CHF is small compared with the scattering of the data.

3.2. Effects of flow parameters on CHF

The left Y-axis in Fig. 5 shows the effect of the inlet water temperature on CHF. Fig. 5 represents the measured CHF with the heated length of 50 mm (a), 100 mm (b), and 200 mm (c), respectively. This figure indicates that the CHF tends to increase with decreasing the inlet water temperature. This tendency becomes large for the short heated length.

In the existing literatures concerning the subcooled boiling CHF, e.g. [15], it is described that the CHF could be correlated with the equilibrium vapor quality at the burnout point and mass velocity well. Since the burnout occurs at the exit of the heated section in most cases of the present experiments, the equilibrium vapor quality at the exit of the heated section when the burnout occurred, $x_{ex,CHF}$ called 'critical quality' below, is also indicated on the right Y-axis in Fig. 5. In case of uniformly heated subcooled boiling CHF, a CHF curve and a heat balance curve intersect in negative thermal quality region as shown in Fig. 6. The thermal quality and heat flux on this intersection are the critical quality, $x_{ex,CHF}$ and CHF, q_{CHF} respectively. The thermal quality, x_{eq} at the flow-directional distance from heated inlet, z, can be generally calculated as follows:

$$x_{eq} = x_{in} + \frac{P_h}{AGh_{fg}} \int_0^z q(z')\,dz', \quad x_{in} = \frac{h_{in} - h_{fsat}}{h_{fg}}. \tag{1}$$

The critical quality for a one-side heated rectangular channel could be calculated by the following equation:

$$x_{ex,CHF} = x_{in} + C^+ Bo, \quad C^+ \equiv \frac{P_h L_h}{A} = \frac{w_h L_h}{ws}$$
$$\left(\text{Tube}: \; C^+ = \frac{4L_h}{D}\right), \; Bo \equiv \frac{q_{CHF}}{Gh_{fg}}. \tag{2}$$

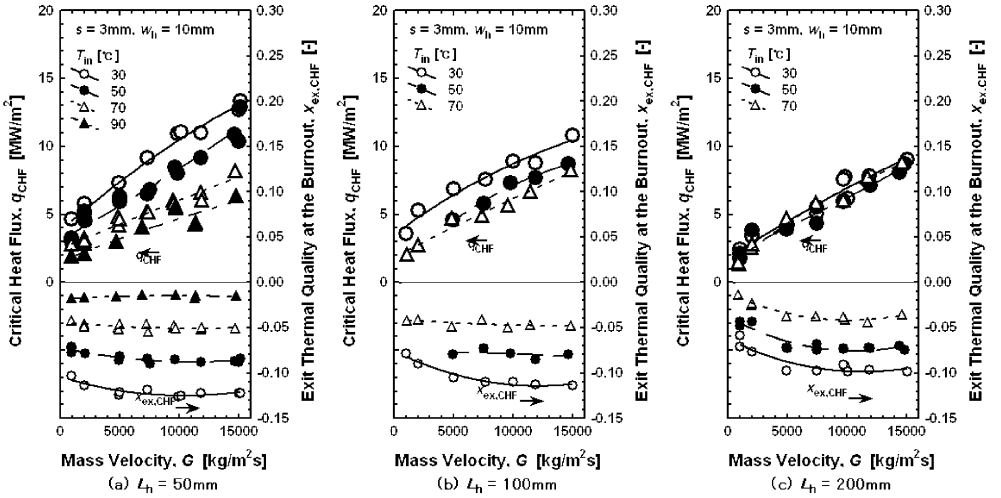

Fig. 5. Effect of inlet water temperature on CHF and critical quality.

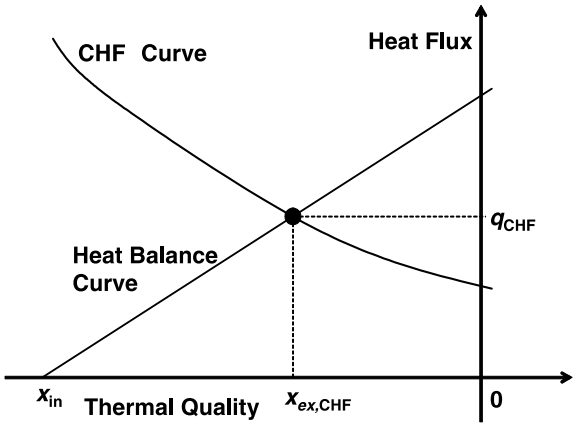

Fig. 6. CHF curve and heat balance curve in subcooled boiling CHF region.

The authors studied the mutual relationship (correlation) between the dimensionless numbers such as Weber number, boiling number *Bo*, and critical quality using the present CHF database and statistical techniques. Dimensionless numbers were selected by dimensional analysis using methods such as Kutateladze, Zenkevich and Katto correlations. It was found from the study that high linearity or good correlation could be seen between a dimensionless CHF parameter K^+ defined by the following equation and critical quality:

$$K^+ \equiv Bo\left(\frac{\text{Viscous force}}{\text{Surface tension}}\right)^{0.5} = Bo\left(\frac{\mu L u}{\sigma L}\right)^{0.5} = Bo(Gv/\sigma)^{0.5}, \quad (3)$$

where Gv/σ is the dimensionless number equal to the ratio of Weber number ($We \equiv \rho u^2 L/\sigma$) to Reynolds number ($Re \equiv uL/v$), ($We/Re$).

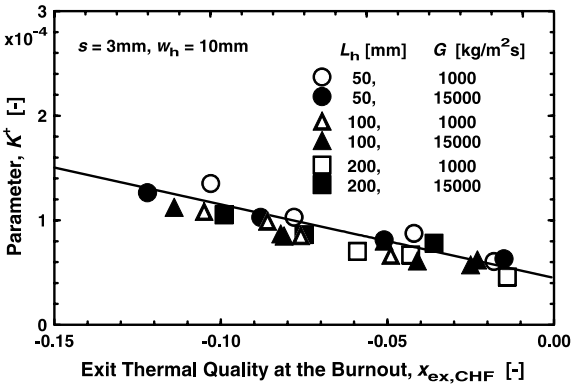

Fig. 7. Correlation between CHF parameter K^+ and critical quality.

Fig. 7 shows the correlation between the CHF parameter K^+ and critical quality. The solid line indicated in Fig. 7 represents the linear least square fit line obtained by all the data with channel gap of 3 mm and heated width of 10 mm. Fig. 7 shows a good correlation between the CHF parameter K^+ and critical quality, and this correlation includes the effects of mass velocity and inlet water temperature on CHF.

3.3. Effects of geometry parameters on CHF

3.3.1. Channel gap

Fig. 8 shows the effects of the channel gap on CHF and critical quality. Critical quality has a tendency to become low when mass velocity is high under the same gap conditions. Effects of channel gap and mass velocity on CHF are small except for the condition of channel gap = 3 mm and mass velocity = 15000 kg/

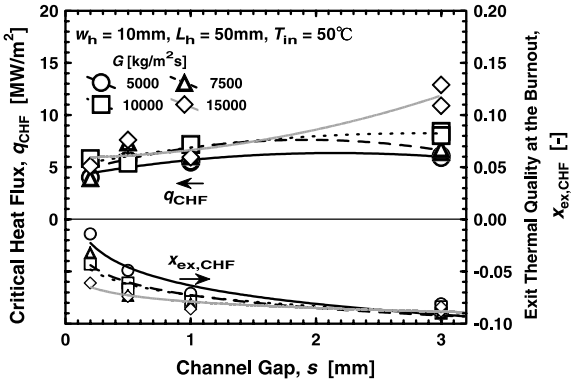

Fig. 8. Effect of channel gap on CHF and critical quality.

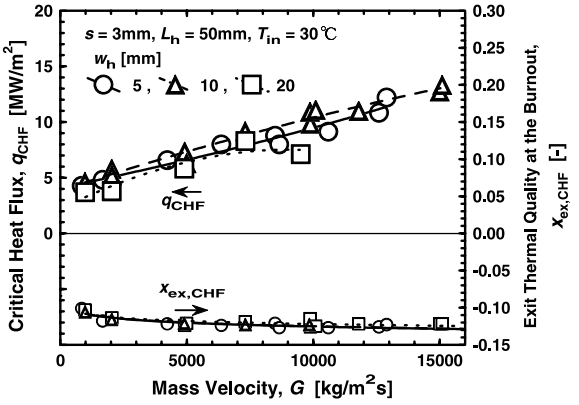

Fig. 10. Effect of heated width on CHF and critical quality.

(m^2 s). Critical quality becomes high for small channel gaps.

The geometric parameter C^+, exit thermal quality and exit water temperature are inversely proportional to the channel gap. Therefore, at first, we thought that boiling begins easily and the generated bubbles rapidly expand in size in case of small channel gaps. As a result, there was the possibility that the CHF would decrease for the small channel gaps. But the CHF measured by the present experiments did not decrease in the test sections with small channel gaps. It was found from photographic observation under CHF conditions [13] that vapor bubble size and density of the bubble at the CHF condition become small for the small channel gap. It was inferred, based on the observation in the test sections with small channel gaps, that tiny vapor bubbles that were generated on the heated surface are strongly influenced by the condensation of subcooled water that flows on the non-heated wall side.

Fig. 9 shows the correlation between the CHF parameter K^+ and critical quality with the channel gap as a parameter. As the linearity between the CHF parameter K^+ and critical quality could be seen in Fig. 9, the correlation can describe the effect of channel gap on CHF.

3.3.2. Heated width

Effects of the heated width on CHF and critical quality are shown in Fig. 10. For the large heated width, the geometry parameter C^+, exit thermal quality and also exit water temperature become high. In case of the present test sections, if the heated width changes from 5 to 20 mm, C^+ changes from 11.9 to 15.2. Therefore, it was inferred that the CHF decreases with increasing the heated width. However, effects of the heated width on CHF and critical quality were small within the scattering of CHF data, which was obtained using the test sections with the heated width/channel width ratio, w_h/w of 0.71–0.91. Fig. 11 shows the correlation between the CHF parameter K^+ and critical quality with the heated width as a parameter. Scattering of the CHF parameter K^+ on the critical quality is small for the heated width of 5–20 mm.

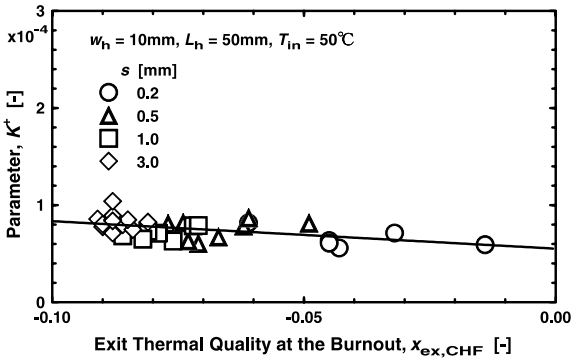

Fig. 9. Correlation between CHF parameter K^+ and critical quality with channel gap as a parameter.

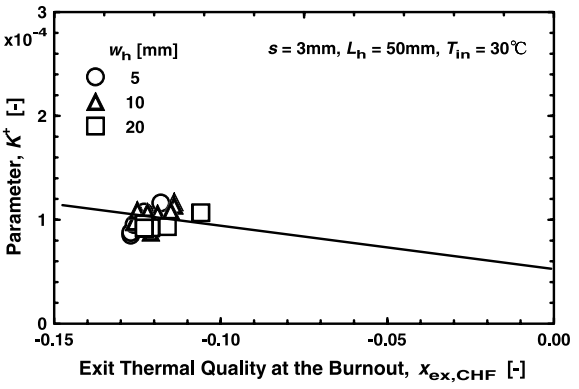

Fig. 11. Correlation between CHF parameter K^+ and critical quality with heated width as a parameter.

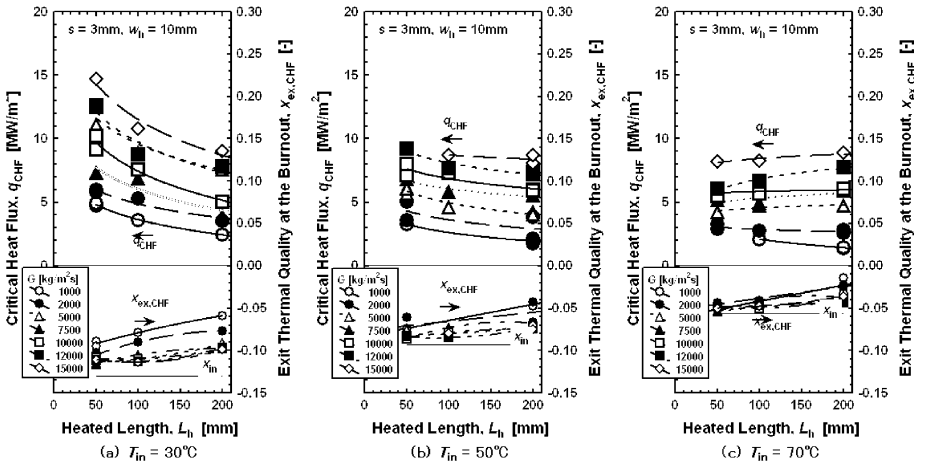

Fig. 12. Effect of heated length on CHF and critical quality.

3.3.3. Heated length

Effects of the heated length on CHF and critical quality were shown in Fig. 12. The CHF increases with decreasing the heated length. This tendency is remarkable for the low inlet water temperature, and the effect of heated length is small in comparison with the scattering of the data at the inlet water temperature = 70 °C. The tendency was similar to that in the small diameter tubes [3]. The critical quality decreases with decreasing the heated length. In case of high inlet water temperature, that is, high inlet quality condition, the critical quality becomes high.

The correlation between the CHF parameter K^+ and critical quality with the heated length as a parameter is shown in Fig. 7. The heated length is included in the thermal quality same as other parameters. As shown in Fig. 7, linearity between the CHF parameter K^+ and critical quality is high, and effect of the heated length could be included in this correlation.

3.4. CHF correlation for one-side heated narrow rectangular channels

Various parameter effects on CHF could be expressed by the correlation between the CHF parameter K^+ and critical quality. Thereupon, all CHF data measured in one-side heated rectangular channels are correlated using the CHF parameter K^+ and critical quality, and the following experimental correlation was conducted:

$$K^+ = C_1(x_{ex,CHF} + C_2), \quad C_1 = -5.173 \times 10^{-4}, \quad C_2 = -0.06921. \tag{4}$$

Calculation accuracy, a standard deviation of $q_{CHF,cal}/q_{CHF,exp}$ ratio, is ±41%. The accuracy could be improved 2–10 times better than the examination using the existing CHF prediction methods for the one-side heated narrow rectangular channels.

4. Discussion of the applicability to other heating geometry channels

Extensibility of the previous correlation, Eq. (4), was investigated using other CHF databases in narrow channels. Fig. 13 shows the correlations using the CHF data in both-side heated narrow rectangular channel [10], half-circumferentially heated tube [11] and full-circumferentially heated tubes [3,4]. In the CHF database obtained in full-circumferentially heated tubes, special CHF data measured in tubes with tube inner diameter ⩽ 3 mm and heated length ⩽ 30 mm is included. In case of the special data, the CHF parameter K^+ tended to scatter about twice more than other general data. The

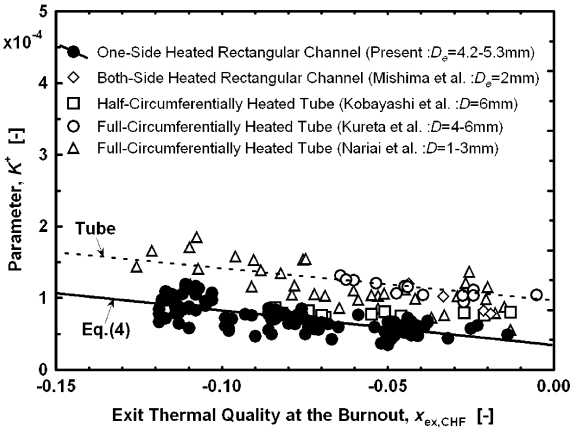

Fig. 13. Correlation between CHF parameter K^+ and critical quality with heating geometry as a parameter.

special CHF data is excluded in Fig. 13, because it was thought that peculiarity of the tubes with very small diameter and very short heated length appeared in such cases. Solid line and dotted line indicated in Fig. 13 represent Eq. (4) and the linear least-square fit line of the full-circumferentially heated tube data, respectively. As shown in Fig. 13, linearity between K^+ and critical quality can also be seen in addition to one-side heated rectangular channels. Experimental data measured in small-diameter tubes tend to scatter under the low critical quality and high CHF conditions. It was found from Fig. 13 that K^+ in tubes becomes large in comparison with that in one-side heated narrow rectangular channels. As for extension of Eq. (4) to other channel geometries, various geometry parameters were investigated by arranging the coefficients C_1 and C_2 in Eq. (4). As a result, a heated perimeter ratio defined by heated perimeter (P_h)/wetted perimeter (P_w) could express the heating geometry effect. Next, coefficients C_1 and C_2 were modified using the heated perimeter ratio in order to predict the CHF not only in one-side heated rectangular channels but also in both-side heated rectangular channels and half- and full-circumferentially heated small-diameter tubes. Modified coefficients C_1 and C_2 are described as follows:

$$C_1 = \left[6.9\left(\frac{P_h}{P_w}\right)^2 - 10\left(\frac{P_h}{P_w}\right) + 2\right] \times 10^{-3},$$
$$C_2 = -0.75\left(\frac{P_h}{P_w}\right)^2 + 0.9\left(\frac{P_h}{P_w}\right) - 0.28. \quad (5)$$

The comparison between the present correlation, $q_{CHF,cal}$, and experimental data, $q_{CHF,exp}$ [3,4,10,11], is shown in Fig. 14. Calculation accuracy of the correlation, a standard deviation of $q_{CHF,cal}/q_{CHF,exp}$, is 45% as indicated by dotted line in Fig. 14. Applicable range of the correlation is within the range of Table 2. Subcooled boiling CHF in one- and both-side heated narrow rectangular channels and half- and full-circumferentially heated small-diameter tubes under atmospheric pressure could be calculated by new dimensionless correlation. The unaccomplished task is to accumulate the high pressure CHF data and to investigate the applicability of the correlation to high pressure in the future works.

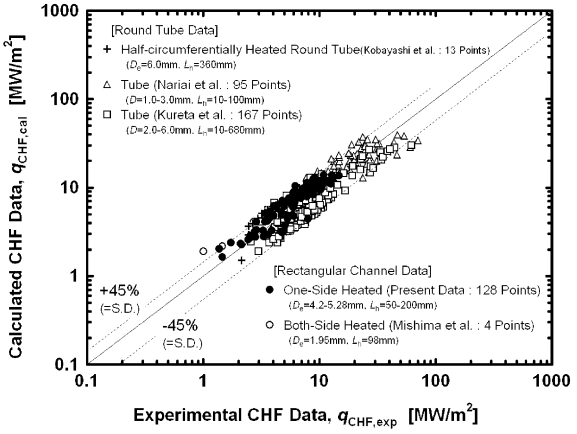

Fig. 14. Comparison of the calculated CHF by the new correlation with the experimental CHF data.

Table 2
Applicable range of the correlation

Parameter	Symbol	Applicable range
Equivalent diameter	D_e	1.0–7.8 mm
Heated perimeter ratio	P_h/P_w	0.25–1.0
Heated length	L_h	10–200 mm
Mass velocity	G	1000–2000 kg/(m^2 s)
Inlet water temperature	T_{in}	5–90 °C
Critical heat flux	q_{CHF}	1.0–70.0 MW/m^2
Critical quality	$x_{ex,CHF}$	−0.163–0.0099

5. Conclusions

CHF experiments in subcooled boiling flow were carried out to conduct a CHF correlation for high-heat-flux components, which work under the one-side heated rectangular cooling condition. The following knowledge was obtained under the present experimental conditions:

(1) CHF does not decrease remarkably with decreasing the channel gap.
(2) Effects of the heated width on CHF and critical quality are small.
(3) Critical quality decreases with decreasing the heated length.
(4) Critical quality increases with increasing the inlet water temperature.
(5) In case of tubes, the dimensionless CHF parameter K^+ tends to have higher value in comparison with that for one-side heated narrow rectangular channels.

New subcooled boiling CHF correlation is proposed for narrow rectangular channels and small-diameter tubes as follows. Calculation accuracy of the correlation is ±45% (maximum 10 times better in comparison with the existing CHF prediction methods which were proposed for the full-circumferentially heated tubes).

$$K^+ \equiv \left(\frac{q_{CHF}}{Gh_{fg}}\right)\left(\frac{G\nu}{\sigma}\right)^{0.5} = C_1(x_{ex,CHF} + C_2),$$

$$C_1 = \left[6.9\left(\frac{P_h}{P_w}\right)^2 - 10\left(\frac{P_h}{P_w}\right) + 2\right] \times 10^{-3},$$

$$C_2 = -0.75\left(\frac{P_h}{P_w}\right)^2 + 0.9\left(\frac{P_h}{P_w}\right) - 0.28.$$

References

[1] H. Akimoto, Y. Ikeda, J. Kusano, Development of thermal design method of rotating target for DT neutron source, JAERI-M, 94-016, 1994 (in Japanese).

[2] The Joint Project Team of JAERI and KEK, The joint project for high-intensity proton accelerators, JAERI-Tech, 2000-003, 2000 (in Japanese).

[3] M. Kureta, K. Mishima, H. Nishihara, Critical heat flux for flow-boiling of water in small-diameter tubes under low-pressure conditions, Trans. JSME (B) 61 (1995) 4109–4116 (in Japanese).

[4] H. Nariai, F. Inasaka, T. Shimura, Critical heat flux of subcooled flow boiling in narrow tube, in: Proceedings of the ASME–JSME Thermal Engineering Joint Conference, Honolulu, USA, 1987.

[5] G.P. Celata, M. Cumo, A. Mariani, M. Simoncini, G. Zummo, Rationalization of existing mechanistic models for the prediction of water subcooled flow boiling critical heat flux, Int. J. Heat Mass Transfer 37-1 (1994) 347–360.

[6] C.L. Vandervort, A.E. Bergles, M.K. Jensen, An experimental study of critical heat flux in very high heat flux subcooled boiling, Int. J. Heat Mass Transfer 37 (1994) 161–173.

[7] Y. Katto, A prediction model of subcooled water flow boiling CHF for pressure in the range 0.1–20 MPa, Int. J. Heat Mass Transfer 35 (1992) 1115–1123.

[8] Y. Sudo, M. Kaminaga, Critical heat flux at high velocity channel flow with high subcooling, Nucl. Eng. Des. 187 (1999) 215–227.

[9] G.P. Celata, M. Cumo, Y. Katto, A. Mariani, Prediction of the critical heat flux in water subcooled flow boiling using a new mechanistic approach, Int. J. Heat Mass Transfer 42 (1999) 1457–1466.

[10] K. Mishima, T. Hibiki, Y. Saito, T. Takeda, Thermal-hydraulic design concept of the N-arena solid-target system in JHF project, in: Proceedings of the International Workshop on JHF Science, Tsukuba, Japan, 1998.

[11] T. Kobayashi, K. Mishima, Heat transfer for flow-boiling of water and critical heat flux in half-heated round tube under low-pressure condition, Trans. JSME (B) 66 (2000) 2150–2156 (in Japanese).

[12] M. Araki, M. Ogawa, M. Akiba, S. Suzuki, Experimental and analytical evaluations on critical heat flux under one side heating condition for fusion applications, Fus. Technol. 21 (1992) 1835–1839.

[13] M. Kureta, H. Akimoto, Experimental study on critical heat flux along one-side heated rectangular channel under subcooled conditions, in: Proceedings of the 6th International Conference on Nuclear Engineering (ICONE-6), CA, USA, 1998, p. 6226.

[14] M. Kureta, H. Akimoto, Critical heat flux of subcooled flow boiling in narrow rectangular channels, in: Proceedings of the 6th International Conference on Nuclear Engineering (ICONE-7), Tokyo, Japan, 1999, p. 7016.

[15] L.S. Tong, Boundary-layer analysis of the flow boiling crisis, Int. J. Heat Mass Transfer 11-7 (1968) 1208–1211.